
Article:
Zhao, Yao, Li, Chuanyang, Li, Dongdong et al. (2 more authors) (2021) Overview of the Optimal Design of the Electrically Excited Doubly Salient Variable Reluctance Machine. Energies. 228. ISSN: 1996-1073

https://doi.org/10.3390/en15010228

---

energies

MDPI

Review

Overview of the Optimal Design of the Electrically Excited Doubly Salient Variable Reluctance Machine

Yao Zhao [1], Chuanyang Lu [1], Dongdong Li [1,*], Xing Zhao [2] and Fan Yang [1]

[1] College of Electric Power Engineering, Shanghai University of Electric Power, Shanghai 200090, China; nihaozhaoyao@163.com (Y.Z.); 18800428295@163.com (C.L.); yangfan@shiep.edu.cn (F.Y.)
[2] Department of Electronic Engineering, University of York, York YO10 5DD, UK; xing.zhao@york.ac.uk
* Correspondence: powerldd@126.com

Abstract: The Electrically Excited Doubly Salient Variable Reluctance Machine (EEDSVRM) is a new type of brushless machine designed according to the principle of air gap reluctance change. There is neither permanent magnet steel nor excitation winding on the rotor. The rotor is made of silicon steel sheets, thus the structure of the variable reluctance machine is very simple. There are many optimization methods for this type of machine optimal design, such as novel machine topology optimization, finite element simulation-based optimization, mathematical analysis-based optimization, intelligent algorithm-based optimization, and multiple fusion-based optimization. Firstly, this article introduces the basic structure and working principle of the EEDSVRM and analyzes both its common regularity and individual difference. Then, the different optimization design methods of EEDSVRM are reviewed, the advantages and disadvantages of the different optimization methods are summarized, and the research interests of the optimization design of variable reluctance machines in the future are prospected.

Keywords: Electrically Excited Doubly Salient Variable Reluctance Machine (EEDSVRM); machine topology; optimization design; finite element simulation; mathematical analysis; intelligent algorithm; multiple fusion

Citation: Zhao, Y.; Lu, C.; Li, D.; Zhao, X.; Yang, F. Overview of the Optimal Design of the Electrically Excited Doubly Salient Variable Reluctance Machine. *Energies* **2022**, *15*, 228. https://doi.org/10.3390/en15010228

Academic Editors: Federico Barrero and Lorand Szabo

Received: 28 November 2021
Accepted: 27 December 2021
Published: 30 December 2021

1. Introduction

Traditional machine excitation sources are concentrated on the rotor, such as the permanent magnet synchronous machine (PMSM), which has a higher power density and efficiency, has attracted much attention, and has been widely used [1]. However, the permanent magnets placed on the rotor usually need to take special reinforcement measures to overcome the centrifugal force during high-speed operation, which leads to a complex machine structure and high manufacturing cost [2]. Moreover, the poor heat dissipation capacity of the machine leads to an increase in the surface temperature of the rotor, which may cause irreversible demagnetization of the permanent magnets. The typical stator electric exciter machine represented by EEDSVRM has received more and more attention in recent years because of its solid structure and high robustness.

There are two kinds of Variable Reluctance Machines (VRMs): unilateral salient pole and bilateral salient pole. The bilateral salient pole VRM is more popular due to its many advantages, such as the largest ratio of maximum to minimum reluctance and better electromechanical energy conversion characteristics. There are three types of EEDSVRM, namely the Wound-field Doubly Salient Machine (WFDSM) [3], Switched Reluctance Machine (SRM) [4], and Electrical Excitation Flux-switching Machine (EEFSM) [5], as shown in Figure 1.

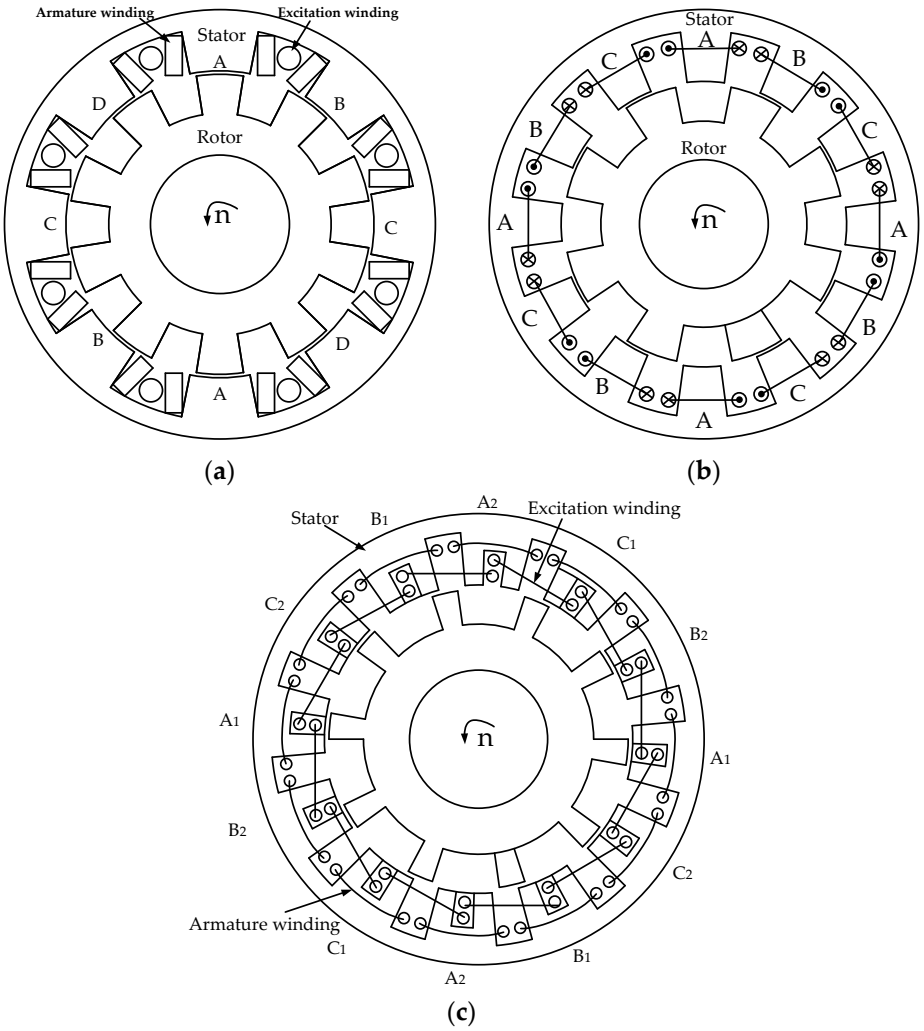

Figure 1. Stator excited VRM. (**a**) WFDSM [3]. (**b**) SRM [4]. (**c**) EEFSM [5].

In recent years, EEDSVRM have attracted increasing attention and become one of the research highlights in the machine field. In [6–12], the control strategy research for EEDSVRM is proposed. Traditional position sensors have many inherent disadvantages, such as increasing the cost of the drive system and reducing the robustness of the machine. In order to improve the overall stability of the WFDSM, a position sensorless control strategy that adopts the relationship between the machine's self-inductance and the rotor position to estimate the rotor position is applied to the WFDSM [6,7]. Aiming at the problem of large torque ripple that is inherent in VRM, an instantaneous torque control strategy incorporating the adaptive terminal sliding mode to suppress SRM torque ripple is proposed [8,9]. An improved direct instantaneous torque control method of the 12/8-pole WFDSM drive system has been researched. The application of this control strategy can reduce the torque ripple of the WFDSM and improve the torque output capability effectively [10]. In [11], a new of fault-tolerant control strategy is proposed for the fault of the power converter. Simulation results show that the proposed fault-tolerant control strategy can effectively alleviate the output performance degradation of WFDSM, caused by power converter failure. In [12], the sliding mode control was applied to the flux-switching machine (FSM), which can improve the stability of the FSM drive system. In [13], the fault characteristics of short circuit and open circuit faults for EEFSM were studied. By changing the switching state of the power transistor, a basic three closed-loop fault-tolerant control strategy based on speed, winding, and current and short-circuit current can be achieved. A fault diagnosis method based on wavelet packet decomposition was introduced for

SRM [14]. The power converter fault diagnosis for WFDSM is proposed in [15]. The control strategy is widely used in VRM as it suppresses the torque ripple, which makes the torque smoother and the overall robustness of VRM improved.

As a new electric excitation machine, EEDSVRM is widely used in popular fields such as aerospace and electric vehicles because of its simple structure and high robustness. However, due to its structural characteristics, VRM has problems such as excessive torque pulsation, which affects operating performance. Therefore, it is necessary to consider the machine structure and optimize the design of the machine to find the optimal combination of structural parameters to make the EEDSVRM achieve the best operating performance, which is of great benefit to the large-scale application of VRM in industry. The optimization design of EEDSVRM ontology was researched in [16–21]. There are many types of EEDSVRM ontology optimization designs, which can be roughly divided into five types: novel machine topology-based optimization, finite element simulation-based optimization, mathematical analysis-based optimization, intelligent algorithm-based optimization, and multiple fusion-based optimization. These five optimization design methods have their own characteristics. It is relatively time-consuming to propose new machine topology optimization and finite element optimization. Although mathematical formula analysis meets the requirements of real-time optimization, the optimization accuracy is still insufficient compared to finite element. Multi-objective optimization using intelligent algorithms can improve optimization efficiency. The optimization method of multiple fusion combines the advantages of multiple optimization methods and greatly improves the optimization efficiency as well as reduces the optimization cost.

In this paper, the topology, working principle and optimization design methods of EEDSVRM are overviewed. In Section 2, the different topological structures of EEDSVRM will be classified, their structural characteristics and working principles are analyzed, and their personality rules and personality characteristics will be summarized. Different optimization design methods for EEDSVRM will be analyzed and summarized in Section 3. In Section 4, the advantages and disadvantages of various optimization design methods are reviewed and the prospects for the optimization design of EEDSVRM in the future are put forward.

2. Basic Topologies, Principles, and Performances

2.1. WFDSM

According to the machine excitation mode, the Doubly Salient Machine (DSM) can be divided into three categories, as follows: the Wound-field Doubly Salient Machine (WFDSM), which is shown in Figure 1a; the Doubly Salient Permanent Magnet Machine (DSPM); and the Hybrid Excitation Doubly Salient Machine (HEDSM), as shown in Figure 2 [22–24]. Compared with DSPM and HEDSM, WFDSM does not use permanent magnets for excitation. Instead, it only relies on the DC power supply to provide the excitation source. In this way, the magnetic flux of the machine can be controlled by adjusting the amplitude of the excitation current and the risk of irreversible demagnetization of the machine can be avoided. Therefore, the WFDSM can be used in harsh environments and has a strong magnetic flux adjustment capability.

The working mode of WFDSM is different from DSPM and HEDSM, which adopt permanent magnet excitation because of the DC excitation mode. When current flows into the excitation winding, a magnetic field is established inside the machine. The magnetic flux generated by the main magnetic field passes through the yoke and magnetic poles of the stator and rotor and penetrates the entire magnetic circuit of the machine. When the machine rotor is driven to rotate by the prime mover, the flux linkage of the armature winding changes with the rotor position, resulting in a symmetrically induced potential. Unlike the permanent magnet excitation, the air gap magnetic field remains constant, which results in poor output voltage regulation and fault demagnetization capabilities. In WFDSM, the main magnetic flux of the machine can be controlled by adjusting the excitation current to affect the output voltage. The external uncontrollable rectifier circuit is

shown in Figure 3 [25], where e_{Af}, e_{Bf}, e_{Cf}, and e_{Df} are the induced voltages of windings A, B, C, and D; W_A, W_B, W_C, and W_D are the windings A, B, C and D; R_A, R_B, R_C, and R_D are the self-resistance of the armature windings of A, B, C, and D; and R is the external load.

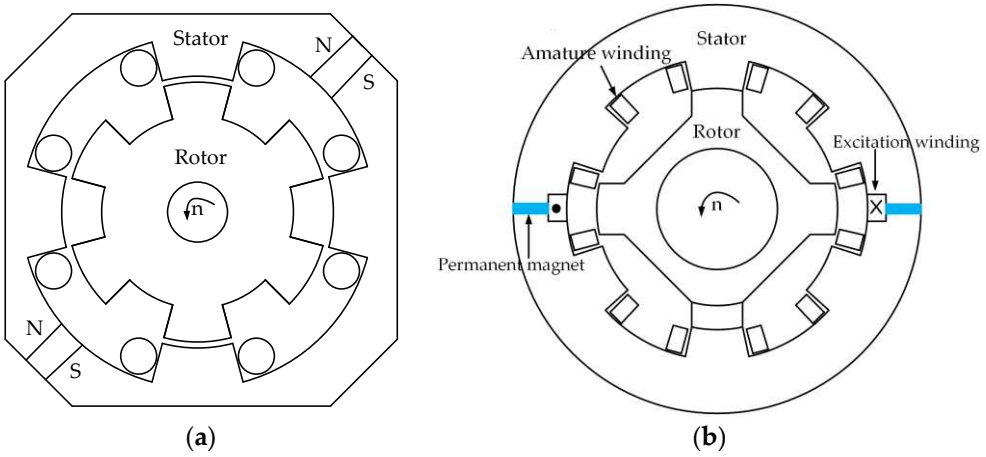

Figure 2. (**a**) DSPM machine [22]. (**b**) HEDSM machine [23].

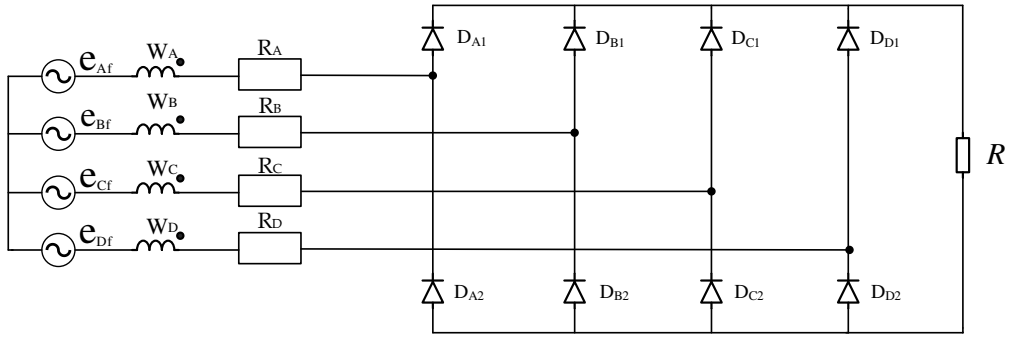

Figure 3. Full bridge rectifier circuit [25].

2.2. SRM

The stator and rotor of SRM are salient pole structures. As shown in Figure 1b, the salient pole of the stator is wound with armature winding, while there is no excitation winding. The magnetic flux moves along the path of minimum reluctance. When the stator and rotor poles are aligned, the air gap reluctance is the smallest. On the contrary, when the cogging is aligned, the air gap reluctance of the machine is the largest. Therefore, SRM follows the principle of minimum reluctance and the magnetic field is distorted to produce electromagnetic torque. Due to its simple structure, stable operation, and wide speed regulation range, it is widely used in aerospace, electric vehicle, and other fields. SRM have two-phase, three-phase, and multi-phase structures, and the stator and rotor also have different pole slot matching combinations. Generally speaking, if the multi-phase structure is adopted, the torque ripple of SRM is relatively small [26]. The relationship between the pole slot and phase number of SRM is as follows:

$$\begin{cases} L_{min}(N_S, N_r) = mN_r \\ L_{min}(N_S, N_r) > N_S > N_r \end{cases} \quad (1)$$

where L_{min} is the least common multiple of the number of poles of the stator and rotor, m is the phase number of SRM, and N_S and N_r represent the number of poles of the stator and rotor, respectively.

The pole slot between the stator and rotor of SRM is shown in Table 1. The most common one is the three-phase 12/8-pole machine, as shown in Figure 1b. Increasing the

number of poles of SRM can reduce the torque ripple and vibration problems caused by SRM to a certain extent [27].

Table 1. Common pole slot fit combination of the stator and rotor of SRM.

m	1	2	3	3	4	5	6
N_S	2	4	6	12	8	10	12
N_r	2	2	4	8	6	8	10

2.3. EEFSM

Identical to the excitation method of DSM, in addition to EEFSM that uses only direct current for excitation, FSM also includes a flux-switching permanent magnet machine (FSPM) that uses permanent magnets for excitation and a hybrid flux-switching machine (HEFSM) in which permanent magnets and direct current are used for excitation at the same time. The topology of FSPM and HEFSM are shown in Figure 4. Although FSPM is considered to be the latest stator excited reluctance machine [28], the permanent magnets used for excitation inevitably encounter demagnetization problems. It is because of the ability to achieve magnetic field adjustment and fault demagnetization under high temperature and harsh operating environments that EEFSM has attracted increasing attention and become one of the research highlights in the VRM field. Figure 1c shows the most widely used 12/10 pole for EEFSM.

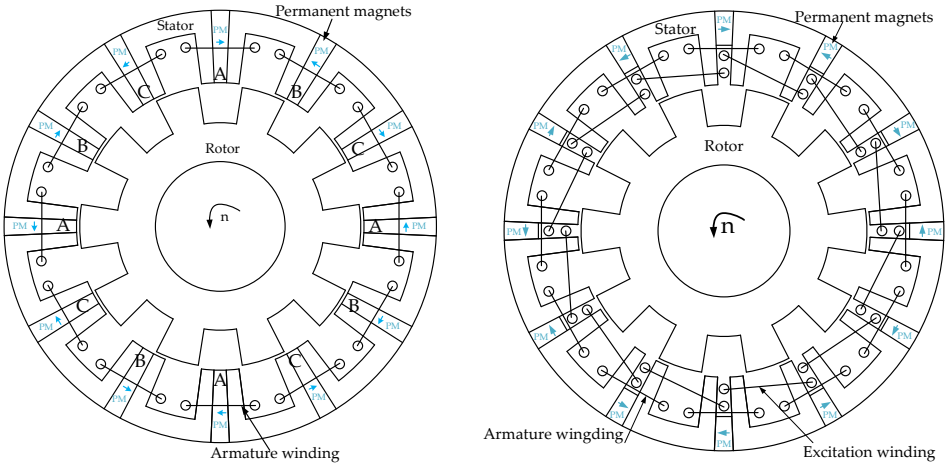

Figure 4. (**a**) FSPM [12]. (**b**) HEFSM [5].

As shown in Figure 1c, it can be seen that there are 12 salient pole silicon steel cores on the stator. Slots are made on the stator teeth and the field windings are embedded in them. The excitation currents of the adjacent two sets of stator slots are opposite to each other.

Compared with conventional SRM, EEFSM can work in a full cycle and both its torque density and power density are higher, which makes it more suitable for applications with high performance requirements such as aerospace and offshore wind power.

With the periodic change of the overlapping area between the rotor pole and stator teeth, the air gap magnetic conductivity in the main magnetic circuit also changes, resulting in the magnetic linkage and back electromotive force in the phase winding, changing with the rotor position, which realizes the so-called "flux switching", as shown in Figure 5. Reasonably designing the pole slot fit of FSPM and optimizing the structural size of the machine can make the waveform of the flux linkage and back EMF close to the sine wave.

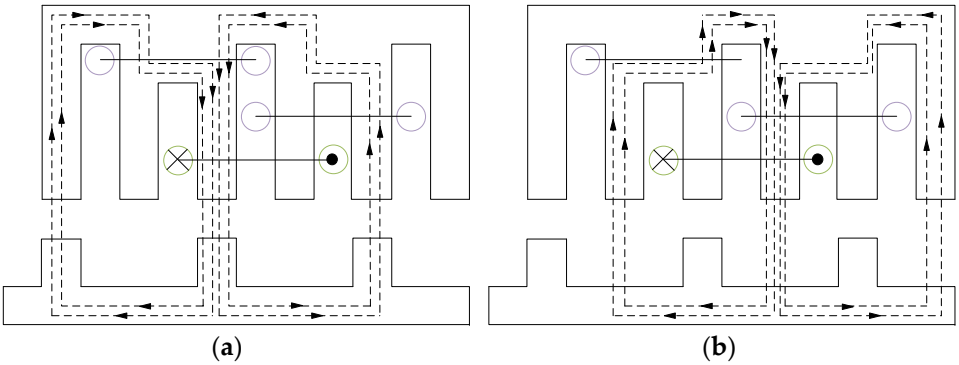

(**a**) (**b**)

Figure 5. (**a**) Maximum forward position of flux linkage. (**b**) Maximum reverse position of flux linkage.

2.4. Dissimilarity and Commonness of the Three Kinds of Variable Reluctance Machines

The three kinds of machines belong to the category of electrically excited variable reluctance machines, which have both dissimilarities and commonness. Commonalities are described below.

(1) Electromagnetic torque is generated by the principle of minimum reluctance.
(2) The stator and rotor adopt salient pole structures, also known as a double salient pole machine. There are no windings on the rotor and both the field winding and armature winding are on the stator poles.
(3) The armature winding of the reluctance machine adopts centralized winding and uses less copper, thus the resistance of the armature winding is relatively small and the copper loss is also small.
(4) All three types of VRM are excited by DC, which avoids the irreversible demagnetization defect of permanent magnet excitation at high temperature.

Furthermore, the three EEDSVRMs of WFDSM, SRM, and EEFSM also have various characteristics. Traditional SRM can only output power when the rotor slides out of the stator poles, while WFDSM and EEFSM can be connected to either a half-bridge rectifier circuit or a full-bridge rectifier circuit. When an external half-bridge rectifier circuit is connected, it can only work when the rotor slides in or slides out of the stator poles, which can only be output in half a cycle. However, when an external full-bridge rectifier circuit is connected, WFDSM and EEFSM will output voltage whether the rotor slides in or slides out of the stator poles. The process that the rotor completes from sliding in to sliding out of the stator poles is called a full cycle. Therefore, SRM can only work in a half cycle, while WFDSM and EEFSM can output power in a full cycle. Compared with WFDSM and EEFSM, the half-cycle working mode makes SRM output power density and torque density at a relatively low rate. Both SRM and WFDSM have unipolar magnetic flux linkage, while EEFSM can switch the magnetic flux to make the magnetic flux linkage present positive and negative bipolarly. Although the excitation windings on WFDSM and EEFSM are both placed on the stator poles, there are still some differences in the placement of the windings. The excitation windings of WFDSM are directly embedded in the stator slots, while EEFSM is slotted on the stator teeth to place the excitation windings.

3. Optimization Design Method

Under certain constraints, the method of improving certain indexes of the machine by changing the structure of the machine is called machine optimization design.

3.1. Novel Machine Topology Optimization

The topology of the machine itself has a great impact on the operation performance of the reluctance machine. Different application fields have different requirements for the topology of the machine. By optimizing the topology, the performance of the VRM can be improved. A new outer rotor WEDSM is proposed, as shown in Figure 6.Compared to the

ordinary WEDSM, it is more suitable for wind power generation because it can improve the output voltage and reduce the ripple due to the realization of bipolar flux and constant self-inductance [29].

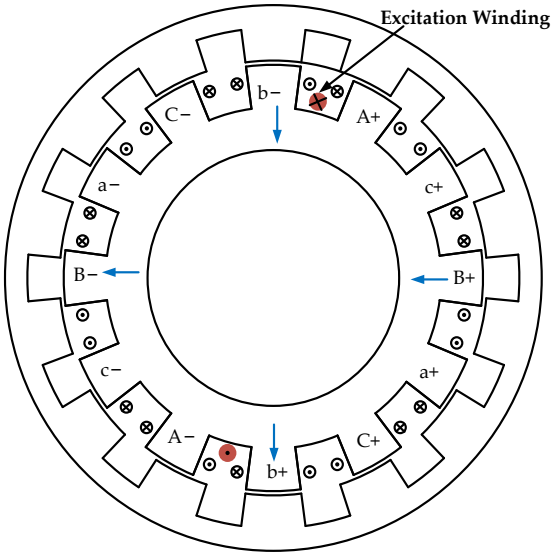

Figure 6. The 12/14 pole outer rotor WEDSM [29].

In order to improve the loss of excitation fault tolerance of WEDSM, a new double stator WEDSM machine combined with the characteristics of SRM is proposed and its inner stator structure is referred to as SRM [30]. The research shows that when an excitation failure occurs, the machine can still continue to work and the torque can remain stable. Unlike traditional SRM, which does not use permanent magnets, permanent magnets are placed on the stator of the new external rotor multi-teeth SRM, as shown in Figure 7. Figure 8 shows the output torque capability of three kinds of machines under different excitation currents; the research shows that this new machine significantly improves the output torque and output power efficiency compared with the SRM without permanent magnets [31–33].

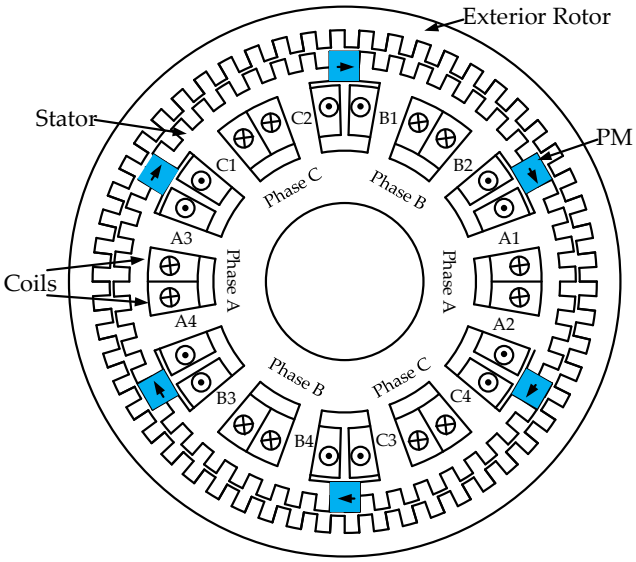

Figure 7. The new external rotor multi-teeth permanent magnet SRM [31].

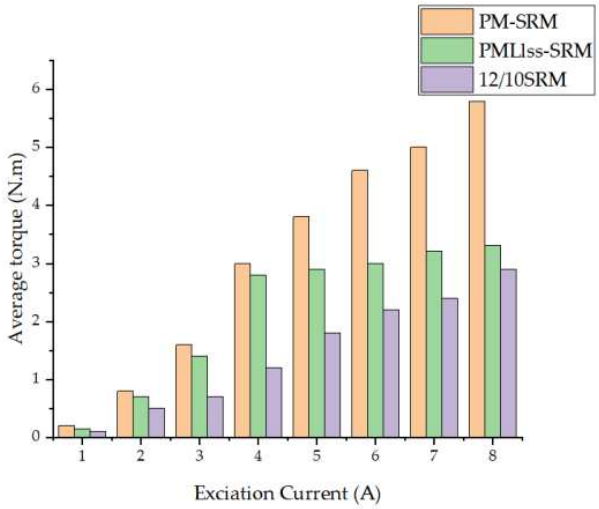

Figure 8. Output torque of three groups of machines under different excitation currents [31].

SRM is widely used in the field of electric vehicles because of its simple manufacture and durability, but its vibration caused by the torque ripple has been criticized. As shown in Figure 9, a double-layer SRM is proposed in [34] to reduce the torque ripple and realize smooth operation of the machine by optimizing the topology of SRM. Not limited to the double-layer structure, a higher-level SRM machine topology is proposed in [35,36]. By adopting an optimized multi-level structure, the torque ripple, vibration, and noise of the SRM are effectively reduced.

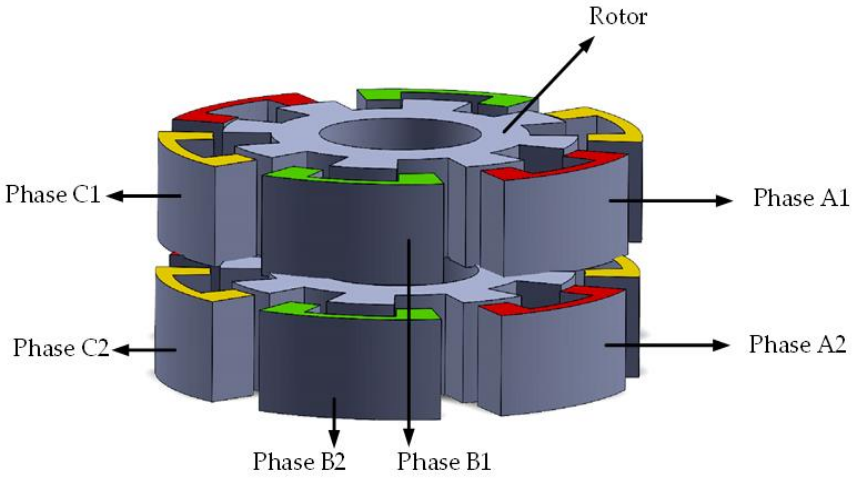

Figure 9. The structure of a double-layer SRM [34].

In addition to multi-layer structure topology optimization, modular and segmented rotor topology are also proposed to optimize SRM so as to reduce the manufacturing cost of the machine and improve both the fault-tolerant performance and torque output capability of SRM. The optimized topology of the modular stator SRM was introduced in [37–40]. The stator is composed of several modular C or E-type silicon steel sheets, as shown in Figure 10. The stator is composed of three groups of completely similar E-type modules in parallel and the module contains three active magnetic poles. Compared with traditional SRM, this type of machine has stronger fault tolerance and higher torque. Since the segmented structure is beneficial to increase the torque and reduce the loss, a novel three-phase segmented stator structure SRM was introduced in [40], as shown in Figure 11, in which two magnetically isolated stator segments form one phase and the windings are wound on it. In addition to the modularization and segmentation of the stator, segmentation of the rotor can also

increase the torque density. A segmented rotor structure SRM is proposed to optimize the machine, as shown in Figure 12; the output torque ripple of the optimized machine is greatly reduced; and the machine noise is also improved [41–49].

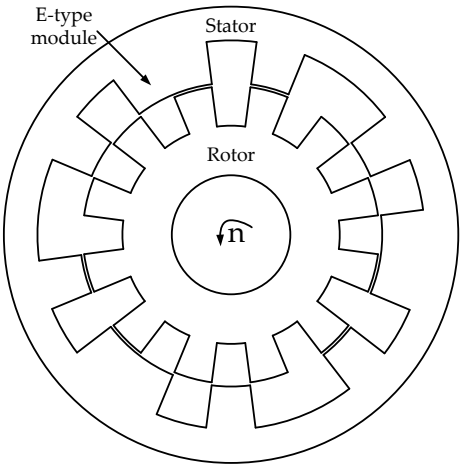

Figure 10. Improved 9/12 pole E-type module SRM [39].

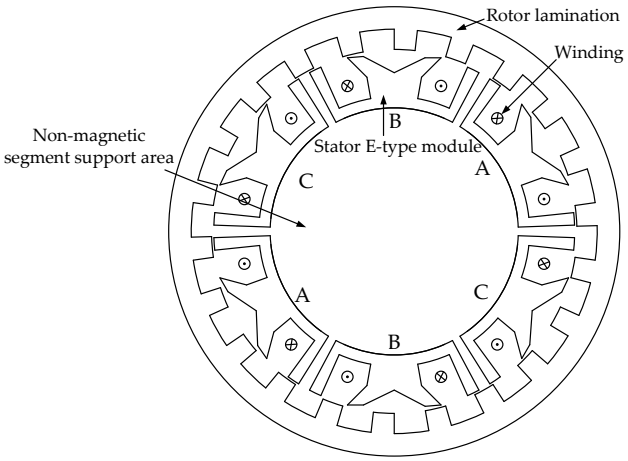

Figure 11. The structure of the segmented stator SRM [40].

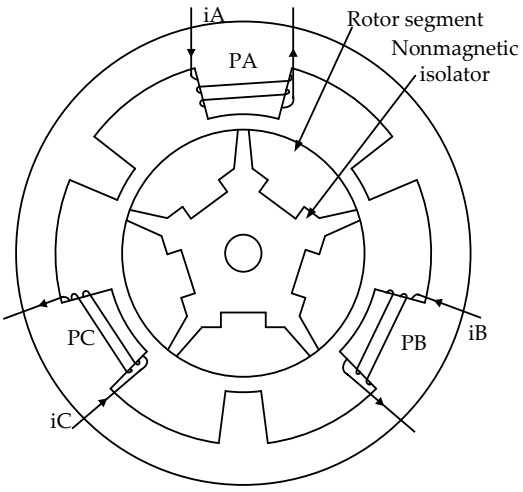

Figure 12. The structure of the segmented rotor SRM [38].

Both the modular stator and segmentation of both the stator and rotor mentioned above are a single optimization of the stator or rotor. The three-phase SRM proposed in [50] is a comprehensive modular machine, which combines the E-type modular stator and segmented rotor. This comprehensive modular structure SRM has better fault tolerance than traditional SRM. An SRM topology with modularity on both armatures is proposed. Multiple sets of C-type modules form a stator and the rotor poles do not have a yoke, as shown in Figure 13. The biggest advantage of this topology is to reduce the mass and it is suitable for both electric vehicles (EVs) and wind power fields with high performance requirements [35]. In [38], an axial flux SRM, in which both the stator and the rotor are made of modules, is proposed. The stator is formed by connecting multiple sets of C-type modules and each module is wound with an armature winding. Experimental research proves that by optimizing the traditional magnetic flux path, the proposed modular SRM has higher efficiency. Furthermore, the robustness and ease of manufacturing make it very suitable for industrial applications. With the upgrading of industrial applications, the performance requirements of the machine are constantly being improved. A comprehensive modular SRM machine with higher output power and stronger robustness is proposed. The stator part of this special integrated modular machine is spliced by six E-type modules and the rotor part is also processed in sections. This special dual modular processing makes it more suitable for high-performance industrial fields, such as EVs and wind power [45].

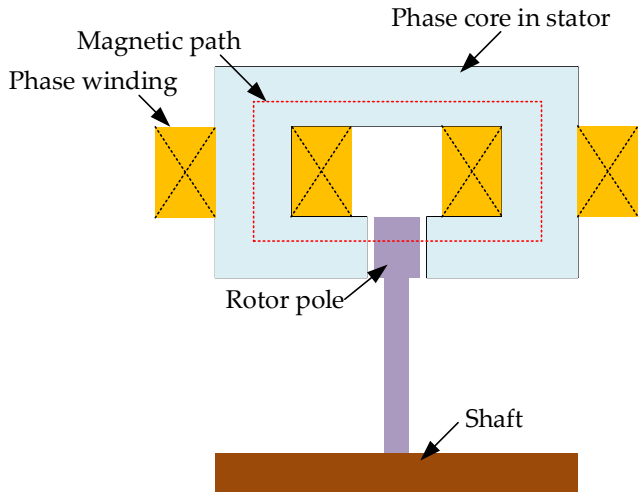

Figure 13. Comprehensive segmented yokeless rotor SRM [35].

3.2. Finite Element Analysis and Design

Different from the above machine, we propose a variety of new machine topologies to optimize the machine, wherein the finite element optimization does not change the reluctance machine topology. Finite element analysis is a currently popular numerical analysis method. First, the solution domain is decomposed into a finite number of smaller intervals. Then, these single cells are solved. Finally, the feasible solution of the entire solution domain can be derived. This method can better deal with complex engineering problems, such as mechanical and electromagnetic problems. In the process of machine optimization, the ANSYS finite element simulation software is used to establish a machine simulation model that needs to be optimized. By changing the structural parameters of the machine for optimization simulation, the most optimal set of structural parameters can be obtained. The finite element simulation is used to optimize the key structural parameters of WEDSM, as shown in Figure 14 and Table 2.

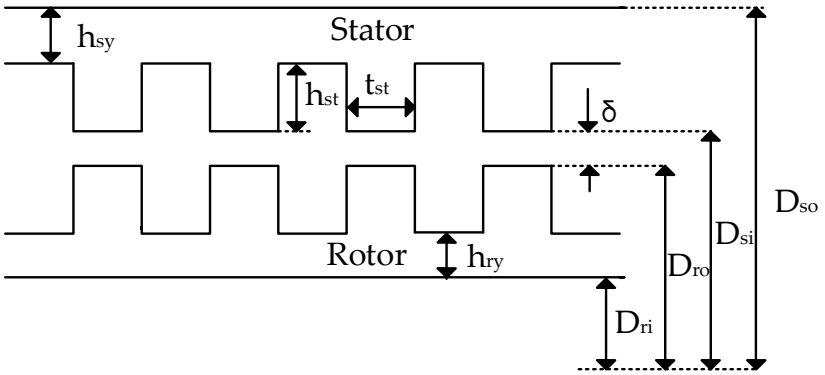

Figure 14. Structure parameters of VRM.

Table 2. Main structural parameters of VRM.

Stator		Rotor	
Outer diameter	D_{SO}	Outer diameter	D_{rO}
Inner diameter	D_{si}	Inner diameter	D_{ri}
Pole height	h_{st}	Pole height	h_{rt}
Yoke height	h_{sy}	Yoke height	h_{ry}
Pole width	t_{st}	Pole width	t_{rt}

The optimal combination is determined to optimize the power generation performance of the machine by FEA [51–53]. To observe the influence of the torque of the stator and rotor pole arc width SRM, in [54], a non-linear model between the motor structure parameters and the output performance is established through ANASY. Based on the model established above, we determined the optimal stator and rotor pole arc width to increase the torque while suppressing torque ripple. Since the stator and rotor adopt a salient pole structure, it will inevitably bring bad problems, such as torque ripple and noise, to the SRM. Notches on the rotor teeth can be used to suppress the torque ripple and the notch shape is shown in Figure 15 [55]. Finite element simulation was used for analysis and it was found that the torque pulsation of SRM reaches the minimum at a notch depth of 2 mm. The influence of the position of the rotor molding clinches on the SRM torque ripple is often ignored. Through finite element simulation and by comparing the influence of the position of the molding clinches on SRM under different currents, it is found that the torque ripple of SRM can be effectively suppressed when molding clinches that are close to the rotor [56]. Through the three-dimensional finite element simulation software, the 12/8 SRM of five different lamination shapes were compared and analyzed, and the best topological shape was sought to minimize vibration and noise [57].

The optimum ratio of the SRM diameter and axial length is established through finite element analysis to improve the torque bulk density [58]. The electromagnetic torque of the SRM is closely related to the phase reluctance and current, while phase reluctance is related to the air gap and rotor. thus the torque ripple can be effectively reduced by optimizing the rotor geometry [59–61]. In the process of machine optimization, multi-level optimization is involved. The first level obtains the maximum torque by optimizing the rotor diameter and air gap, and the second level of optimization, namely the higher harmonics appearing in the machine, is reduced by optimizing the width of the stator teeth and permanent magnets [62]. The effects of the stator and rotor tooth width, permanent magnet thickness on the electromagnetic torque, and levitation force of the bearing-less FSRM are studied by finite element simulation, and the optimization of the two indexes are obtained at the same time. Figure 16 shows the comparison diagram of the machine harmonics before and after optimization, in which the fifth and seventh harmonics are greatly reduced. The results show that the optimized parameters improve the machine performance significantly [63].

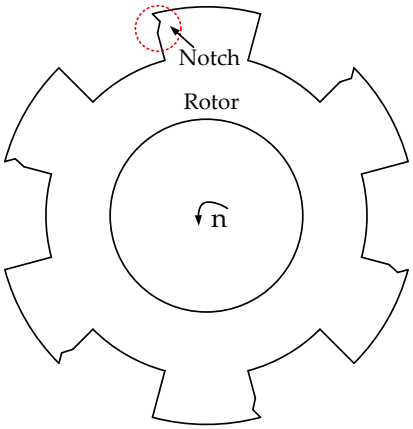

Figure 15. The notch of the rotor pole [55].

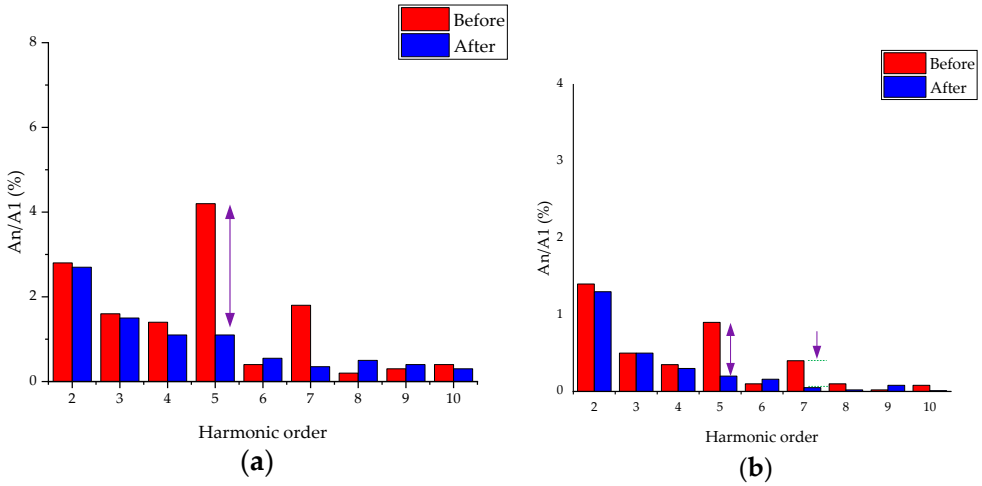

Figure 16. Harmonic analysis diagram [63]. (**a**) Permanent magnetic flux. (**b**) Back-EMF.

In the process of the multi-parameter and multi-objective optimization of the machine, 11 groups of geometry structure parameters can be transformed into two virtual representatives by coordinate transformation and then different objectives can be optimized by finite element simulation. In this way, the simulation time is greatly reduced compared to the finite element simulation of the 11 groups of body structure parameters [64].

When too many structural parameters need to be optimized at the same time, the parameters can be grouped to discuss the impact on the target performance. The stator teeth and rotor section, stator shunt ratio, and rotor section height can be combined to seek the optimization of the Embedded Segmented Rotor Flux-switching Machine (ESRFSW) electromagnetic performance.

3.3. Mathematical Analytical Optimization

The geometric parameters of the reluctance machine have a great impact on the machine performance, thus the optimal parameters can be found through finite element simulation to optimize the machine performance, but this method is time-consuming and cannot meet the real-time requirements. Thus, an analytical method using mathematical equations to express the machine performance is proposed to find the optimal parameters of the machine. This method can identify the relationship between each group of structural parameters and the machine output performance directly and clearly. In [65], the In-Wheel Switched Reluctance Machine (IW-SRM) is taken as an example to find out the analytical equation between each group of structure parameters and the output performance. The machine size analytical equation solved by MATLAB is used to find the target optimal

solution. When a set of parameter solutions are obtained, the accuracy of the parameters is verified by finite element simulation.

As the reluctance machine is developed based on the magnetic field modulation theory, the mathematical analytical formula can be established through the magnetic field modulation theory to optimize the machine pole slot in order to meet the requirements of optimizing the machine performance [65–67].

The principle of the SRM torque generation is studied from the perspective of air gap modulation theory. The magnetic conductivity model of SRM and the mathematical analytical model of magnetic field modulation are established, and the influence of the corresponding magnetic field harmonic order on the output torque is analyzed. Finally, the torque performance of the machine is optimized based on the above analysis [66].

The three-phase current flowing into the SRM stator can be divided into the DC component and AC component:

$$\left\{\begin{array}{l} I_a(t) = \left\{\begin{array}{ll} I_{amp} & a_{on} < \omega t < a_{off} \\ 0 & else \end{array}\right\} \\ I_b(t) = \left\{\begin{array}{ll} I_{amp} & a_{on} < \omega t - \frac{2\pi}{mN_r} < a_{off} \\ 0 & else \end{array}\right\} \\ I_c(t) = \left\{\begin{array}{ll} I_{amp} & a_{on} < \omega t - \frac{4\pi}{mN_r} < a_{off} \\ 0 & else \end{array}\right\} \end{array}\right\} \quad (2)$$

The m, N_r, ω, and I_{amp} in Formula (2) are the phase number of the SRM, the number of rotor poles, the angular velocity, and the current amplitude, respectively. α_{on} and α_{off} represent the conduction angle and cut-off angle of the phase current. Fourier series is used to expand Formula (2):

$$\left\{\begin{array}{l} I_a(t) = I_{dc} + \sum\limits_{j=1,2,3\ldots}^{\infty} I_j \cos[j\omega t - \varphi_j] \\ I_b(t) = I_{dc} + \sum\limits_{j=1,2,3\ldots}^{\infty} I_j \cos[j(\omega t - \frac{2\pi}{3}) - \varphi_j] \\ I_c(t) = I_{dc} + \sum\limits_{j=1,2,3\ldots}^{\infty} I_j \cos[j(\omega t + \frac{2\pi}{3}) - \varphi_j] \end{array}\right\} \quad (3)$$

The I_{dc} appearing in Formula (3) is the fundamental DC component and I_j and φ_j represent the current amplitude and phase angle of the jth harmonic, respectively [66]. The Fourier series is used to decompose the SRM winding current into two parts, namely the fundamental DC and AC harmonics. The two currents together constitute the stator magnetomotive force of the SRM. Due to the unique double salient pole structure of SRM, the salient pole effect of the stator and rotor must be considered in the air gap magnetic field modulation theory. Since the concentrated winding in SRM is wound on the stator side, the winding function brought by the salient poles of the stator can be expressed by Formula (4) [66]:

$$\left\{\begin{array}{l} W_a(\theta) = \sum\limits_{h=1,3,5\ldots}^{\infty} \frac{4N_a}{h\pi} K_{\omega h} \cos[\frac{N_c}{2m} h\theta] \\ W_a(\theta) = \sum\limits_{h=1,3,5\ldots}^{\infty} \frac{4N_a}{h\pi} K_{\omega h} \cos[\frac{N_c}{2m} h(\theta - \frac{2\pi}{3})] \\ W_a(\theta) = \sum\limits_{h=1,3,5\ldots}^{\infty} \frac{4N_a}{h\pi} K_{\omega h} \cos[\frac{N_c}{2m} h(\theta + \frac{2\pi}{3})] \end{array}\right\} \quad (4)$$

In Formula (4), W_a represents the stator winding function, Na is the number of the connected turns of each phase of the SRM, and Nc is the number of stator coils [66]. The winding factor of SRM is represented by KW. In the SRM air gap permeability analysis,

an energy wave containing a DC component will be caused by the SRM rotor with salient poles, as shown in Formula (5):

$$P(\theta, t) = \sum_{k=0,1,2\ldots}^{\infty} P_k \cos[kN_r(\theta - \theta_0 - \Omega_r t)] \tag{5}$$

In Formula (5), the amplitude of the air gap permeance is represented by P_k The magnetomotive force of SRM is obtained by multiplying the phase current, represented by Formula (3), and the stator winding function, represented by Formula (4), as shown in Formula (6):

$$\left\{ \begin{array}{l} F_{dc}(\theta) = [W_a(\theta) + W_b(\theta) + W_c(\theta)]I_{dc} \\ F_{abc}(\theta.t) = W_a(\theta)(I_a(t) - I_{dc}) + W_b(\theta)(I_b(t) - I_{dc}) + W_c(\theta)(I_c(t) - I_{dc}) \end{array} \right\} \tag{6}$$

In Formula (6), F_{dc} represents the DC-induced electromotive force and the AC-induced electromotive force is represented by F_{abc} The air gap field in Formula (7) can be obtained by Formulas (6) and (5).

$$\left\{ \begin{array}{l} B_{dc}(\theta, t) = F_{dc}(\theta)P(\theta, t) \\ B_{abc}(\theta, t) = F_{abc}(\theta)P(\theta, t) \end{array} \right\} \tag{7}$$

In Formula (7), B_{dc} and B_{abc} are used to express the air gap magnetic flux density caused by the DC and AC magnetomotive force. The above two sets of different air gap magnetic densities can be multiplied to obtain the SRM torque expression, as shown in Formula (8):

$$T = P \times \frac{\pi g r L}{\mu_0} B_{dc} \times B_{abc} \tag{8}$$

In Formula (8), P is used to indicate the number of pole pairs. The μ_0 at the position of the denominator is a constant, which is used to represent the magnetic permeability in vacuum; g and r on the numerator are used to indicate the length and radius of the SRM air gap; and L indicates the stack length of SRM. In Formula (8), it can be clearly seen that the torque of SRM is not only related to the inherent structural parameters of the machine itself, but also closely related to two different induced electromotive forces generated by AC and DC. Using the mathematical analytical formula of the above analysis, the two air-gap magnetic fields of AC and DC can be adjusted reasonably so that the torque pulsation can be effectively suppressed while the torque of SRM is increased [66].

Based on the deduced mathematical expressions of the back EMF and the torque of the FSM, the effects of the rotor pole number, pole arc, and permanent magnet thickness on the back EMF are studied. According to the analytical expression, the FSM is optimized to minimize the torque ripple and maximize the torque density [67].

3.4. Intelligent Algorithm Optimization

In the process of machine design optimization, a variety of optimization indexes and structural parameters are needed to be considered together. The efficiency is very low by using the traditional finite element and mathematical analysis methods. With the development of artificial intelligence and machine learning, an optimization method for a reluctance machine based on intelligent algorithms is proposed.

SRM is widely used in electric vehicles and other fields because of its simple manufacturing and durability, and multiple indicators such as torque, efficiency, and cost are required at the same time in consideration of the SRM design. In [68], a global optimization method based on the multi-objective optimization algorithm is proposed, with stator and rotor poles as parameter variables. The high torque, low copper consumption, and high torque density are chosen as three groups of optimization objectives. The specific optimization process is shown in Figure 17 and the research results show that this method has a shorter optimization time and higher precision.

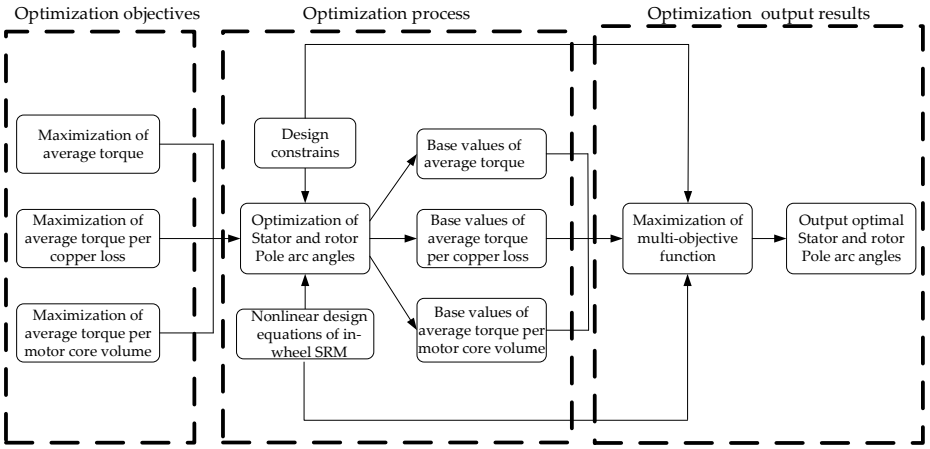

Figure 17. Multi-objective optimization flow chart [68].

In addition to the multi-objective optimization algorithm mentioned above, there are many kinds of intelligent algorithms applied in SRM [68–77]. Compared to the ordinary gradient descent method, the genetic algorithm (GA) can converge faster, thus it is used in high-speed SRM optimization [69]. With the progress of algorithm technology, the optimization convergence of GA in the field of multi-structure parameters is still unsatisfactory. Based on this, the simulated annealing algorithm (SA) is proposed to compare to the genetic algorithm. The results show that the SA has initially reached convergence after evolution of 10%, but the GA still does not reach convergence after evolution of 40%, as shown in Figure 18. The results prove that the SA has higher convergence in the multi-objective optimization of the reluctance machine [70].

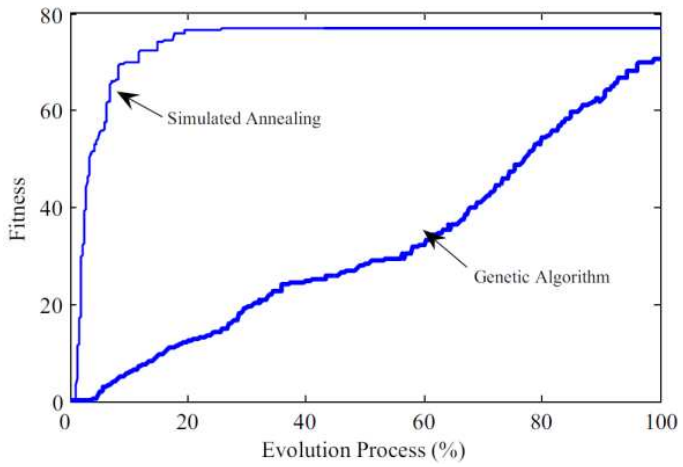

Figure 18. Multi-objective optimization evolutionary process of GA and SA [70].

According to the actual design requirements, the simulation model of the electric vehicle is established in MATLAB and the geometric parameters related to SRM are optimized by the Taguchi–chicken swarm optimization algorithm (Taguchi-CSO) [72].

Before the intelligent algorithm is used, not only the finite element simulation is used to optimize the machine, but also the design of the experiment (DOE) and stochastic evolution are used to optimize the reluctance machine. Taking the DOE as an example, it is a mathematical statistical method about the mapping between reaction structure parameters and optimization indexes. It is often used for machine optimization but, once again, two structural parameters are involved, thus the number of experiments will be very large and the optimization efficiency low. Therefore, a new optimization method of the reluctance machine based on the combination of mathematical statistics and intelligent algorithms is

proposed in [73]. This design method can be widely used to collect global information of the reluctance machine and to improve the optimization efficiency [74–76].

Represented by DOE and the differential evolution algorithm (DEA), a machine optimization method combining mathematical statistics and intelligent algorithms is proposed and the specific optimization process is shown in Figure 19. DOE mathematical statistics is carried out firstly, which can effectively screen out the structural parameters with high sensitivity to machine cost, torque ripple, and other optimization objectives. Candidate design variables are greatly reduced and construct the response surface (RS) between high-sensitivity parameters and optimization indexes. The parameter model constructed by RS is globally optimized by using the DEA to obtain the optimal solution.

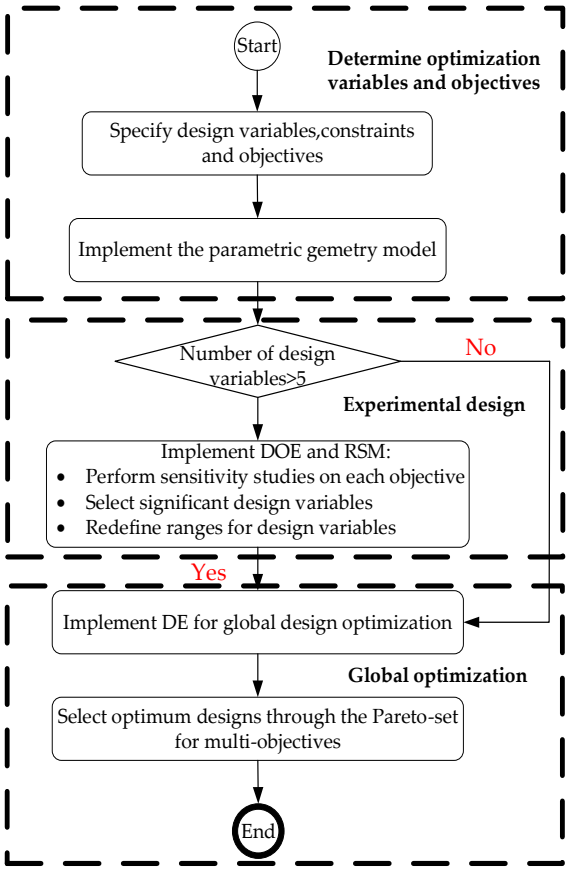

Figure 19. Machine optimization process based on DOE and DE [71].

However, the accuracy of the second-order RS model constructed by DOE will decrease with the increasement of the design structural parameters, which will make the mapping relationship between structural parameters and optimization objectives unreal. Therefore, a high-dimensional mapping relationship must be established. In [75], Audze–Eglais Latin hypercube designs (AELHD) are proposed to replace DOE to establish a third-order RS model and then Particle Swarm Optimization (PSO) is used to find the three-objective optimal solutions of SRM with maximum torque, maximum efficiency, and minimum torque ripple.

When there are few machine design parameters, the mathematical statistics of the experimental design can be used to establish the RS analysis model to reflect the mapping relationship between structural parameters and optimization objectives. However, when too many candidate design variables need to be considered, the efficiency of this method is particularly low. In order to improve the multi-objective optimization efficiency of FSM, a multi-level optimization method is proposed; the specific optimization flow chart is shown in Figure 20.

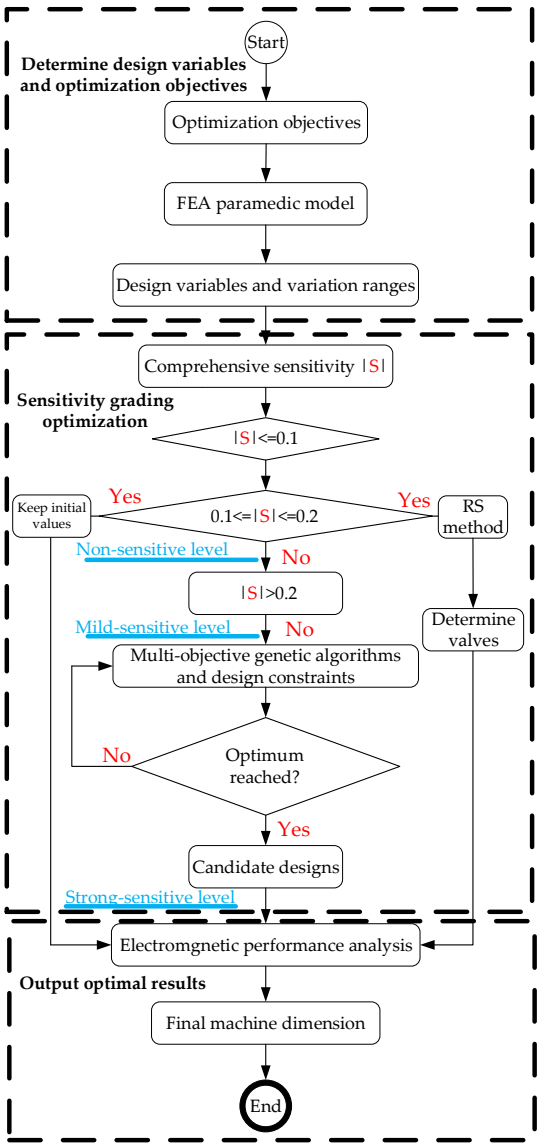

Figure 20. Sensitivity grading optimization flow chart [76].

Firstly, the torque, torque ripple, and low-magnetic coupling between the inner and outer machines are determined as the optimization objectives of the brushless double-mechanical port flux-switching machine (BDMP-FSM) and then the sensitivity analysis of machine structural parameters are carried out to determine both the high-sensitivity parameters and general-sensitivity parameters for the optimization objectives. The sensitivity level is used for classification and the non-sensitivity parameters are directly excluded. The sensitivity parameters are four groups of variables and the RS model can be used. The high-sensitivity parameters have eight groups of variables. The multi-objective genetic algorithm (MOGA) is used to find the optimal solution. This layered design method can effectively reduce the optimization time and improve the optimization efficiency [76].

3.5. Multivariate Fusion Optimization

The above optimization methods of the reluctance machine are based on a single optimization method. With the improvement of the performance requirements of the reluctance machine, a multivariate fusion optimization method with higher accuracy and efficiency is proposed. It combines the above optimization methods so that the optimized machine can be suitable for the complex and changeable working environment.

Topology optimization combined with intelligent algorithm optimization is proposed in [40,78–81]. Considering that the topology of SRM using permanent magnets can improve the output torque, a new hybrid excitation SRM is proposed. The biggest feature of this machine is to place the permanent magnet on the adjacent stator pole of SRM. The stator pole saturation is reduced to improve the output torque. However, in order to obtain the best performance, GA is integrated to optimize the machine parameters to achieve the maximum output torque [78]. Moreover, the SRM topology with the segmented stator structure can also be used to improve the SRM torque performance. By introducing this new machine topology, combined with the multi-element fusion optimization of the intelligent algorithm optimization of key parameters, the stator-segmented SRM shows better torque density than the conventional SRM and is suitable for the field of electric vehicles (EVs) with high demand for torque density [40].

An optimization method of the reluctance machine combining magnetic field modulation theory and the intelligent optimization algorithm is proposed. Through the magnetic field modulation theory and winding function analysis of WEDSM, the optimal pole slot coordination of the stator and rotor is sought so as to achieve the optimal no-load back EMF and winding inductance. Then, taking the output voltage and fault tolerance as the optimization objectives, GA is used to globally optimize the key structural parameters of the WEDSM. The finite element simulation and experimental results show that the multi-element fusion optimization method combined with magnetic field modulation theory and intelligent algorithms has higher optimization efficiency [82].

A multiple optimization method combining mathematical analysis and the intelligent optimization algorithm is proposed to reduce SRM torque ripple. Through the analysis of SRM vibration characteristics, the mathematical analysis model of its torque and radial force is established, and then the DE intelligent algorithm is used to optimize the Fourier series, representing the phase current characteristics, so as to seek to minimize the torque ripple and vibration of the SRM. The research results show that this multivariate fusion optimization method greatly reduces the calculation time and improves the optimization efficiency compared to the single use of FEA [83]. The machine model is very important for multivariate fusion optimization. A generalized machine mathematical analysis model based on Maxwell's equations is proposed [84]. Through this model, the basic electromagnetic characteristics can be quickly calculated and the design variables used for the multi-objective optimization of the PSO intelligent algorithm are greatly reduced. In this new type of the machine optimization design method, mathematical analysis models and intelligent algorithms are used in combination, which greatly improves the efficiency of SRM's multi-objective optimization design.

Torque ripple and vibration noise have always been the inherent drawbacks of SRM. The traditional optimization method has always been to seek optimization on the machine structure to suppress torque pulsation. However, the torque ripple of SRM is not only restricted by the structure of the machine body, but is also related to the control mode of the machine. In [85,86], a multivariate fusion control method combined with intelligent algorithms is proposed to suppress the torque ripple and vibration noise of SRM. Adaptive sliding mode control is adopted as the control strategy of SRM. Elitist-mutated multi-objective particle swarm optimization is used to optimize a variety of control parameters globally to improve the response of the control system, to increase the robustness of the system, and to finally alleviate the torque ripple of SRM. This kind of control strategy combined with the intelligent optimization algorithm has a higher control efficiency and better effect.

4. Discussion

Compared with traditional rotor-excited machines such as PMSM, the EEDSVRMs represented by WFDSM, SRM, and EEFSM reviewed in this article have no windings wound on the rotor and all windings are concentrated on the wound on the stator, thus the three types of machines are simple in structure and easy to manufacture. In addition, permanent

magnets are not used in the above three types of machines but consider the use of a DC power supply to excite the machines. This unique excitation method enables WFDSM, SRM, and EEFSM to avoid the irreversible demagnetization phenomenon that may be caused by the use of permanent magnets and cause the machine to fail to work normally, which greatly improves the robustness of the machine. With the above advantages, EEDSVRMs represented by WFDSM, SRM, and EEFSM are popular in high-performance industrial applications such as aerospace, EVs, and offshore wind power.

In order to optimize a single goal or multiple goals of the machine, different optimization methods are proposed for EEDSVRM, such as optimization based on new machine topology, optimization based on finite element simulation, optimization based on mathematical formula analysis, optimization based on the intelligent algorithm, and multiple fusion optimization. Various optimization design methods of EEDSVRM have their own characteristics. In order to optimize a certain performance of the machine, it can be considered from the machine topology. For example, a new type of machine topology can be proposed to optimize the original machine according to the needs of industrial applications. The advantage of this method is that it can fundamentally achieve the optimization requirements, but the shortcomings are also obvious because this method, based on the proposed new machine topology optimization, requires in-depth research on the machine body structure, which takes a long time and is relatively inefficient. With the widespread application of industrial finite element simulation software, a method for optimizing motors based on finite element simulation software is proposed. The simulation model of EEDSVRM can be established with limited finite element simulation software and the goal of optimizing the machine can be achieved through the simulation analysis of key structural parameters. The advantage of this optimization method is the high calculation accuracy. However, the disadvantage is that only the discrete geometric parameters of EEDSVRM are compared and analyzed. The sample selected by this method is relatively small and it is impossible to build all models within a feasible range. Real-time optimization cannot be met and this method of optimization requires a lot of time. For example, 2D models take half an hour, while 3D models take longer. The mathematical analysis method is a VRMs-optimization design method based on Maxwell's equations and the air gap magnetic field modulation theory. Although this method meets the subsequent real-time requirements, its calculation process is solved under ideal electromagnetic conditions and many actual electromagnetic effects are ignored, thus its disadvantage is that the accuracy of the calculation results is relatively low. Therefore, the result of the subsequent optimization process may not be the global optimal structural parameter set.

With the popularization of computers and intelligent algorithms, a method to optimize the design of EEDSVRM using intelligent algorithms is proposed. In the process of using intelligent algorithms to optimize the design of EEDSVRM, the whole process is divided into two steps. Firstly, the global optimization method based on DOE and intelligent algorithms uses the experimental design to establish the large data machine parameter model within the feasible range. Then, intelligent algorithms are used under constraints to find the optimal solution that satisfies the optimization goal. Compared with mathematical analysis methods, this optimization method using intelligent algorithms is more efficient and accurate, and can better meet the requirements of the rapid optimization of VRM.

With the wide application of EEDSVRM in high-performance fields such as aerospace and electric vehicles, higher design requirements are put forward in the process of machine optimization design. A global optimization method based on multiple fusion is proposed. This new type of the EEDSVRM optimization design method can integrate the various optimization design methods mentioned above and the advantages of the different optimization methods that have been merged can be absorbed. Therefore, the optimization efficiency of this multiple-integrated optimization design method is higher and the optimization effect is more obvious, which represents the direction of the global optimization of variable reluctance machines in the future.

Author Contributions: Conceptualization, Y.Z. and C.L.; methodology, Y.Z.; validation, Y.Z. and X.Z.; formal analysis, D.L.; investigation, F.Y.; resources, Y.Z.; data curation, X.Z.; writing—original draft preparation, Y.Z. and C.L.; writing—review and editing, Y.Z. and C.L.; visualization, X.Z.; supervision, D.L.; funding acquisition, Y.Z. All authors have read and agreed to the published version of the manuscript.

Funding: This research was funded by Shanghai Rising-Star Program under Grant No. 21QC1400200, Natural Science Foundation of Shanghai under Grant No. 21ZR1425400, Shanghai Science and Technology Project under Grant No.20142202600.

Institutional Review Board Statement: Not applicable.

Informed Consent Statement: Not applicable.

Data Availability Statement: Not applicable.

Conflicts of Interest: The authors declare no conflict of interest.

Nomenclature

AELHD	Audze–eglais latin hypercube designs
BDMP-FSM	brushless double-mechanical port flux-switching machine
DEA	differential evolution algorithm
DOE	design of experiment
DSM	doubly salient machine
DSPM	doubly salient permanent magnet machine
EEDSVRM	electrically excited doubly salient variable reluctance machine
EEFSM	electrical excitation flux-switching machine
ESRFSW	embedded segmented rotor flux-switching machine
EVs	electric vehicles
FSM	flux-switching machine
FSPM	flux-switching permanent magnet machine
GA	genetic algorithm
HEDSM	hybrid excitation doubly salient machine
HEFSM	hybrid flux-switching machine
IW-SRM	in-wheel switched reluctance machine
MOGA	multi-objective genetic algorithm
PMSM	permanent magnet synchronous machine
PSO	particle swarm optimization
RS	response surface
SA	simulated annealing algorithm
SRM	switched reluctance machine
Taguchi-CSO	Taguchi–chicken swarm optimization algorithm
VRM	variable reluctance machine
WFDSM	wound-field doubly salient machine

References

1. Chau, K.T.; Chan, C.C.; Liu, C. Overview of Permanent-Magnet Brushless Drives for Electric and Hybrid Electric Vehicles. *IEEE Trans. Ind. Electron.* **2008**, *55*, 2246–2257. [CrossRef]
2. Tong, W.; Li, S.; Pan, X.; Wu, S.; Tang, R. Analytical Model for Cogging Torque Calculation in Surface-Mounted Permanent Magnet Motors with Rotor Eccentricity and Magnet Defects. *IEEE Trans. Energy Convers.* **2020**, *35*, 2191–2200. [CrossRef]
3. Zhao, Y.; Teng, D.; Li, D.; Zhao, X. Comparative Research on Four-Phase Dual Armature-Winding Wound-Field Doubly Salient Generator With Distributed Field Magnetomotive Forces for High-Reliability Application. *IEEE Access* **2021**, *9*, 12579–12591. [CrossRef]
4. Ferková, Ž.; Suchý, Ľ.; Bober, P. Comparison of 6/4 and 12/8 Switched Reluctance Motor Models Using Direct Torque Control with Torque Lookup Table. *Electr. Eng.* **2019**, *102*, 75–83. [CrossRef]
5. Gaussens, B.; Hoang, E.; Lecrivain, M.; Manfe, P.; Gabsi, M. A Hybrid-Excited Flux-Switching Machine for High-Speed DC-Alternator Applications. *IEEE Trans. Ind. Electron.* **2014**, *61*, 2976–2989. [CrossRef]
6. Zhou, X.; Zhou, B.; Wei, J. A Novel Position-Sensorless Startup Method for DSEM. *IEEE Trans. Ind. Appl.* **2018**, *54*, 6101–6109. [CrossRef]

7. Zhou, X.; Zhou, B.; Wang, K. Position Sensorless Control for Doubly Salient Electromagnetic Machine with Improved Startup Performance. *IEEE Trans. Ind. Electron.* **2019**, *67*, 1782–1791. [CrossRef]
8. Sun, X.; Feng, L.; Diao, K.; Yang, Z. An Improved Direct Instantaneous Torque Control Based on Adaptive Terminal Sliding Mode for a Segmented-Rotor SRM. *IEEE Trans. Ind. Electron.* **2020**, *68*, 10569–10579. [CrossRef]
9. Zhang, X.; Yang, Q.; Ma, M.; Lin, Z.; Yang, S. A Switched Reluctance Motor Torque Ripple Reduction Strategy with Deadbeat Current Control and Active Thermal Management. *IEEE Trans. Veh. Technol.* **2020**, *69*, 317–327. [CrossRef]
10. Chen, X.; Zhang, Z.; Yu, L.; Bian, Z. An Improved Direct Instantaneous Torque Control of Doubly Salient Electromagnetic Machine for Torque Ripple Reduction. *IEEE Trans. Ind. Electron.* **2021**, *68*, 6481–6492. [CrossRef]
11. Hu, D.; Bo, Z.; Gan, Z.; Huang, X.; Zhou, X. Research of Fault-Tolerant Strategy for Power Converter of Four-Phase Dsem Drive. In Proceedings of the 2016 19th International Conference on Electrical Machines and Systems (ICEMS), Chiba, Japan, 13–16 November 2016.
12. Yuan, X.; Wei, Z.; Feng, Y.; Gu, W. Sliding Mode Control of Axial Field Flux-Switching Permanent Magnet Machine. In Proceedings of the 2017 20th International Conference on Electrical Machines and Systems (ICEMS), Sydney, NSW, Australia, 11–14 August 2017.
13. Lin, F.; Chau, K.T.; Lee, C.H.T.; Liu, C. Fault Signature of a Flux-Switching DC-Field Generator. *IEEE Trans. Magn.* **2015**, *51*, 1.
14. Gan, C.; Wu, J.; Yang, S.; Hu, Y.; Cao, W. Wavelet Packet Decomposition-Based Fault Diagnosis Scheme for SRM Drives with a Single Current Sensor. *IEEE Trans. Energy Convers.* **2015**, *31*, 303–313. [CrossRef]
15. Feng, X.; Zhou, B.; Zhou, X.; Ge, W.; Wang, K. A Novel Fault Diagnosis Method for Power Converter of Doubly Salient Electro-Magnetic Motor. In Proceedings of the 2019 22nd International Conference on Electrical Machines and Systems (ICEMS), Harbin, China, 11–14 August 2019.
16. Pan, Z.; Fang, S.; Lin, H.; Yang, H.; Xue, S. A New Double-Sided Flux Reversal Arc Permanent Magnet Machine With Enhanced Torque Density Capability. *IEEE Trans. Magn.* **2019**, *55*, 1–6. [CrossRef]
17. Gao, Y.; Li, D.; Qu, R.; Jian, L. Design Procedure of Flux Reversal Permanent Magnet Machines. *IEEE Trans. Ind. Appl.* **2017**, *53*, 4232–4241. [CrossRef]
18. Bobba, D.; Bramerdorfer, G.; Sarlioglu, B. A Low-Pole Split Magnet Flux Switching Permanent Magnet Machine with Minimized Harmonic Distortion in Flux Linkage for High Speed Operation. In Proceedings of the 2016 XXII International Conference on Electrical Machines (ICEM), Lausanne, Switzerland, 4–7 September 2016.
19. Abdeen, H.; Varró, D.; Sahraoui, H.; Nagy, A.S.; Debreceni, C.; Hegedüs, Á.; Horváth, Á. Multi-Objective Optimization in Rule-Based Design Space Exploration. In Proceedings of the 29th ACM/IEEE International Conference on Automated Software Engineering, Västerås, Sweden, 15–19 September 2014.
20. Zhao, X.; Niu, S. Design and Optimization of a Novel Slot-PM-Assisted Variable Flux Reluctance Generator for Hybrid Electric Vehicles. *IEEE Trans. Energy Convers.* **2018**, *33*, 2102–2111. [CrossRef]
21. Zhao, X.; Niu, S.; Zhang, X.; Fu, W. Flux-Modulated Relieving-DC-Saturation Hybrid Reluctance Machine with Synthetic Slot-PM Excitation for Electric Vehicle In-Wheel Propulsion. *IEEE Trans. Ind. Electron.* **2021**, *68*, 6075–6086. [CrossRef]
22. Zhang, L.; Wu, L.J.; Huang, X.; Fang, Y.; Lu, Q. A Novel Structure of Doubly Salient Permanent Magnet Machine in Square Envelope. *IEEE Trans. Magn.* **2019**, *55*, 1–5. [CrossRef]
23. He, M.; Xu, W. Novel 6/7 Stator/Rotor Hybrid Excitation Doubly Salient Permanent Magnet Machine. *IEEE Trans. Magn.* **2016**, *52*, 1–5.
24. Wang, S.; Zhang, X.; Zhao, X.; Niu, S.; Fu, W. A Novel Slot-PM Assisted Complementary-Rotor Doubly-Salient Machine with Enhanced Torque Performance. *IEEE Trans. Ind. Electron.* **2021**. [CrossRef]
25. Zhao, Y.; Wang, H.; Li, D.; Qian, R. Comparative Research of a Wound-Field Doubly Salient Generator with Different Rectifiers. *IEEE Trans. Ind. Inform.* **2018**, *14*, 4851–4863. [CrossRef]
26. Wang, C.; Zhang, Z.; Liu, Y.; Geng, W.; Gao, H. Effect of Slot-Pole Combination on the Electromagnetic Performance of Ironless Stator AFPM Machine With Concentrated Windings. *IEEE Trans. Energy Convers.* **2020**, *35*, 1098–1109. [CrossRef]
27. Faiz, J.; Shahgholian, G.; Ghazizadeh, H. Analysis of Dynamic Behavior of Switched Reluctance Motor-Design Parameters Effects. In Proceedings of the Melecon 2010—2010 15th IEEE Mediterranean Electrotechnical Conference, Valletta, Malta, 26–28 April 2010.
28. Mashhadifarahani, F.; Siadatan, A.; Karamalian, D.; Majidi, B.; Ghadimi, A. Designing and Optimization of 9/12 Stator Permanent Magnet Srm to Improve Torque Ripple. In Proceedings of the 2019 IEEE 28th International Symposium on Industrial Electronics (ISIE), Vancouver, BC, Canada, 12–14 June 2019.
29. Wei, J.D.; Bo, Z.; Cheng, F.S.; Zhang, Z.R.; Wu, X. A New Three-Phase Doubly Salient Electrical Magnet Generator for Direct-Driven Wind Power Generation. In Proceedings of the International Conference on Electrical Machines & Systems, Wuhan, China, 17–20 October 2008.
30. Jiang, S.; Zhou, B.; Xiong, L.; Wang, K. Analysis and Design of a Novel Dual-Stator DSEM for Fault-Tolerant Operation Under Loss of Excitation. In Proceedings of the 2020 23rd International Conference on Electrical Machines and Systems (ICEMS), Hamamatsu, Japan, 24–27 November 2020.
31. Farahani, E.F.; Kondelaji, M.A.J.; Mirsalim, M. A New Exterior-Rotor Multiple Teeth Switched Reluctance Motor With Embedded Permanent Magnets for Torque Enhancement. *IEEE Trans. Magn.* **2020**, *56*, 1–5. [CrossRef]

32. Ding, W.; Hu, Y.; Fu, H.; Chen, Q. Analysis and Evaluation of Modular E-Shaped Stator Switched Reluctance Machines Employing Segmented and Conventional Rotor Topologies. *IET Electr. Power Appl.* **2016**, *10*, 939–951. [CrossRef]
33. Farahani, E.F.; Kondelaji, M.A.J.; Mirsalim, M. An Innovative Hybrid-Excited Multi-Tooth Switched Reluctance Motor for Torque Enhancement. *IEEE Trans. Ind. Electron.* **2021**, *68*, 982–992. [CrossRef]
34. Vatani, M.; Mirsalim, M.; Vaez-Zadeh, S. A New Double-Layer Switched Reluctance Motor with a Low Torque Ripple. In Proceedings of the 2019 27th Iranian Conference on Electrical Engineering (ICEE), Yazd, Iran, 30 April–2 May 2019.
35. Xue, X.D.; Cheng, K.W.E.; Bao, Y.J.; Leung, P.L.; Cheung, N. Switched Reluctance Generators with Hybrid Magnetic Paths for Wind Power Generation. *IEEE Trans. Magn.* **2012**, *48*, 3863–3866. [CrossRef]
36. Afjei, E.; Siadatan, A.; Torkaman, H. Magnetic Modeling, Prototyping, and Comparative Study of a Quintuple-Set Switched Reluctance Motor. *IEEE Trans. Magn.* **2015**, *51*, 1–7. [CrossRef]
37. Ruba, M.; Viorel, I.; Szabó, L. Modular Stator Switched Reluctance Motor for Fault Tolerant Drive Systems. *IET Electr. Power Appl.* **2013**, *7*, 159–169. [CrossRef]
38. Labak, A.; Kar, N.C. Designing and Prototyping a Novel Five-Phase Pancake-Shaped Axial-Flux SRM for Electric Vehicle Application Through Dynamic FEA Incorporating Flux-Tube Modeling. *IEEE Trans. Ind. Appl.* **2013**, *49*, 1276–1288. [CrossRef]
39. Eskandari, H.; Mirsalim, M. An Improved 9/12 Two-Phase E-Core Switched Reluctance Machine. *IEEE Trans. Energy Convers.* **2013**, *28*, 951–958. [CrossRef]
40. Mousavi-Aghdam, S.R.; Feyzi, M.R.; Bianchi, N.; Morandin, M. Design and Analysis of a Novel High-Torque Stator-Segmented SRM. *IEEE Trans. Ind. Electron.* **2016**, *63*, 1458–1466. [CrossRef]
41. Widmer, J.D.; Martin, R.; Mecrow, B.C. Optimisation of an 80kW Segmental Rotor Switched Reluctance Machine for Automotive Traction. In Proceedings of the 2013 International Electric Machines & Drives Conference, Chicago, IL, USA, 12–15 May 2013.
42. Xu, Z.; Lee, D.-H.; Ahn, J.-W. Design and Operation Characteristics of a Novel Switched Reluctance Motor with a Segmental Rotor. *IEEE Trans. Ind. Appl.* **2016**, *52*, 2564–2572. [CrossRef]
43. Bilgin, B.; Emadi, A.; Krishnamurthy, M. Comprehensive Evaluation of the Dynamic Performance of a 6/10 Srm for Traction Application in Phevs. *IEEE Trans. Ind. Electron.* **2013**, *60*, 2564–2575. [CrossRef]
44. Vandana, R.; Fernandes, B.G. Design Methodology for High-Performance Segmented Rotor Switched Reluctance Motors. *IEEE Trans. Energy Convers.* **2015**, *30*, 11–21.
45. Ding, W.; Hu, Y.; Wang, T.; Yang, S. Comprehensive Study of Modular E-Core Stator Hybrid-Flux Switched Reluctance Motors with Segmented and Non-Segmented Rotors. *IEEE Trans. Energy Convers.* **2016**, *32*, 382–393. [CrossRef]
46. Szabo, L. A Survey on Modular Variable Reluctance Generators for Small Wind Turbines. *IEEE Trans. Ind. Appl.* **2019**, *55*, 2548–2557. [CrossRef]
47. Bo, W.; Lee, D.H.; Lee, C.W.; Ahn, J.W. Characteristics Analysis of a Novel Segmental Rotor Axial Field Switched Reluctance Motor with Single Teeth Winding. *J. Power Electron.* **2014**, *14*, 852–858.
48. Madhavan, R.; Fernandes, B.G. Axial Flux Segmented SRM With a Higher Number of Rotor Segments for Electric Vehicles. *IEEE Trans. Energy Convers.* **2013**, *28*, 203–213. [CrossRef]
49. Powell, D.J.; Jewell, G.W.; Calverley, S.D.; Howe, D. Iron Loss in a Modular Rotor Switched Reluctance Machine for the \"More-Electric\" Aero-Engine. *IEEE Trans. Magn.* **2005**, *41*, 3934–3936. [CrossRef]
50. Diko, M.; Rafajdus, P.; Makys, P.; Dubravka, P.; Szabo, L.; Ruba, M. A Novel Concept of Short-Flux Path Switched Reluctance Motor for Electrical Vehicles. *Adv. Electr. Electron. Eng.* **2015**, *13*, 206–211. [CrossRef]
51. Zhang, Z.; Sun, L.; Yan, Y. Brushless Doubly Salient Machines with Stator Field Winding for DC Power Generation Applications. In Proceedings of the IECON 2013—39th Annual Conference of the IEEE Industrial Electronics Society, Vienna, Austria, 10–13 November 2013.
52. Yu, Z.; Zhang, Z.; Yin, W.; Li, Y. Influence of Rotor Pole Arc on Generating and Motoring Performance of Doubly Salient Electro-Magnetic Machines. In Proceedings of the 2014 17th International Conference on Electrical Machines and Systems (ICEMS), Hangzhou, China, 22–25 October 2014.
53. Deng, F.; Meng, X.; Xu, L.; Liu, Z. Optimization Design of Doubly Salient Electro-Magnetic Motor under Fault-Tolerant Operation of Excitation Fault. In Proceedings of the 2020 15th IEEE Conference on Industrial Electronics and Applications (ICIEA), Kristiansand, Norway, 9–13 November 2020.
54. Sahraoui, H.; Zeroug, H.; Toliyat, H.A. Switched Reluctance Motor Design Using Neural-Network Method with Static Finite-Element Simulation. *IEEE Trans. Magn.* **2007**, *43*, 4089–4095. [CrossRef]
55. Lee, J.W.; Kim, H.S.; Kwon, B.I.; Kim, B.T. New Rotor Shape Design for Minimum Torque Ripple of Srm Using Fem. *IEEE Trans. Magn.* **2004**, *40*, 754–757. [CrossRef]
56. Sahin, C.; Amac, A.; Karacor, M.; Emadi, A. Reducing Torque Ripple of Switched Reluctance Machines by Relocation of Rotor Moulding Clinches. *IET Electr. Power Appl.* **2012**, *6*, 753–760. [CrossRef]
57. Cai, W.; Pillay, P.; Tang, Z.; Omekanda, A. Low-Vibration Design of Switched Reluctance Motors for Automotive Applications Using Modal Analysis. *IEEE Trans. Ind. Appl.* **2003**, *39*, 971–977. [CrossRef]
58. Goto, H.; Murakami, S.; Ichinokura, O. Design to Maximize Torque-Volume Density of Axial-Flux SRM for in-Wheel EV. In Proceedings of the IECON 2015—41st Annual Conference of the IEEE Industrial Electronics Society, Yokohama, Japan, 9–12 November 2015.

59. Yao, S.; Zhang, W. Optimum Design of 4/3 Srm for Fuel Pump in Hev Considering Output Torque and Vibration. In Proceedings of the Vehicle Power & Propulsion Conference, Hangzhou, China, 17–20 October 2016.
60. Kabir, M.A.; Husain, I. Segmented Rotor Design of Concentrated Wound Switched Reluctance Motor (Srm) for Torque Ripple Minimization. In Proceedings of the 2016 IEEE Energy Conversion Congress and Exposition (ECCE), Milwaukee, WI, USA, 18–22 September 2016.
61. Gundogmus, O.; Elamin, M.; Yasa, Y.; Husain, T.; Sozer, Y.; Kutz, J.; Tylenda, J.; Wright, R. Acoustic Noise Mitigation of Switched Reluctance Machines with Windows on Stator and Rotor Poles. *IEEE Trans. Ind. Appl.* **2020**, *56*, 3719–3730. [CrossRef]
62. Gruber, W. Geometry Optimization of a Bearingless Flux- Switching Slice Motor. In Proceedings of the Electric Machines & Drives Conference, Coeur d'Alene, ID, USA, 10–13 May 2015.
63. Jia, H.; Luo, J.; Cai, J.; Jia, Z.; Cao, Y.; Cheng, M. Optimization Design and Analysis of a Bearingless Flux-Switching Permanent Magnet Machine. In Proceedings of the 2017 IEEE 12th International Conference on Power Electronics and Drive Systems (PEDS), Honolulu, HI, USA, 12–15 December 2017.
64. Guo, K.; Guo, Y. Optimization Design of a Flux Switching Linear Rotary Permanent Magnet Machine. In Proceedings of the 2019 22nd International Conference on Electrical Machines and Systems (ICEMS), Harbin, China, 11–14 August 2019.
65. Yildirim, M.; Polat, M.; Öksüztepe, E.; Omac, Z.; Yakut, O.; Eren, H.; Kaya, M.; Kurum, H. Designing In-Wheel Switched Reluctance Motor for Electric Vehicles. In Proceedings of the 2014 16th International Power Electronics and Motion Control Conference and Exposition, Antalya, Turkey, 21–24 September 2014.
66. Hua, H.; Hua, W.; Zhao, G.; Cheng, M. Torque Production Mechanism of Switched Reluctance Machines with Air-Gap Field Modulation Principle. *IEEE Trans. Energy Convers.* **2020**, *35*, 1617–1627. [CrossRef]
67. Yang, H.; Zhu, Z.Q.; Lin, H.; Xu, P.L.; Zhan, H.L.; Fang, S.; Huang, Y. Design Synthesis of Switched Flux Hybrid-Permanent Magnet Memory Machines. *IEEE Trans. Energy Convers.* **2016**, *32*, 65–79. [CrossRef]
68. Xue, X.D.; Cheng, E.K.W.; Ng, T.W.; Cheung, N.C. Multi-Objective Optimization Design of In-Wheel Switched Reluctance Motors in Electric Vehicles. *IEEE Trans. Ind. Electron.* **2010**, *57*, 2980–2987. [CrossRef]
69. Raminosoa, T.; Blunier, B.; Fodorean, D.; Miraoui, A. Design and Optimization of a Switched Reluctance Motor Driving a Compressor for a PEM Fuel-Cell System for Automotive Applications. *IEEE Trans. Ind. Electron.* **2010**, *57*, 2988–2997. [CrossRef]
70. Jonathan, D.; Bruno, D.; Hamid, B.A. Simulated Annealing and Genetic Algorithms in Topology Optimization Tools: A Comparison through the Design of a Switched Reluctance Machine. In Proceedings of the SPEEDAM 2010, Pisa, Italy, 14–16 June 2010.
71. Peng, Z.; Dan, M.I.; Demerdash, N.A.O. Morphing Parametric Modeling and Design Optimization of Spoke and V-Type Permanent Magnet Machines by Combined Design of Experiments and Differential Evolution Algorithms. In Proceedings of the Energy Conversion Congress & Exposition, Denver, CO, USA, 15–19 September 2013.
72. Chen, H.; Yan, W.; Gu, J.J.; Sun, M. Multiobjective Optimization Design of a Switched Reluctance Motor for Low-Speed Electric Vehicles with a Taguchi–Cso Algorithm. *IEEE/ASME Trans. Mechatron.* **2018**, *23*, 1762–1774. [CrossRef]
73. Mo, L.; Zhang, T.; Lu, Q. Design and Analysis of an Outer-Rotor-Permanent-Magnet Flux-Switching Machine for Electric Vehicle Applications. *IEEE Trans. Appl. Supercond.* **2019**, *29*, 1–5. [CrossRef]
74. Ren, Z.; Zhang, D.; Koh, C.-S. Multi-Objective Worst-Case Scenario Robust Optimal Design of Switched Reluctance Motor Incorporated with FEM and Kriging. In Proceedings of the 2013 International Conference on Electrical Machines and Systems (ICEMS), Busan, Korea, 26–29 October 2013.
75. Ma, C.; Qu, L. Multiobjective Optimization of Switched Reluctance Motors Based on Design of Experiments and Particle Swarm Optimization. *IEEE Trans. Energy Convers.* **2015**, *30*, 1144–1153. [CrossRef]
76. Xiang, Z.; Zhu, X.; Quan, L.; Du, Y.; Zhang, C.; Fan, D. Multilevel Design Optimization and Operation of a Brushless Double Mechanical Port Flux-Switching Permanent-Magnet Motor. *IEEE Trans. Ind. Electron.* **2016**, *63*, 6042–6054. [CrossRef]
77. Zhu, X.; Fan, D.; Mo, L.; Chen, Y.; Quan, L. Multiobjective Optimization Design of a Double-Rotor Flux-Switching Permanent Magnet Machine Considering Multimode Operation. *IEEE Trans. Ind. Electron.* **2018**, *66*, 641–653. [CrossRef]
78. Zhu, J.; Cheng, K.W.E.; Xue, X. Design and Analysis of a New Enhanced Torque Hybrid Switched Reluctance Motor. *IEEE Trans. Energy Convers.* **2018**, *33*, 1965–1977. [CrossRef]
79. Chen, Y.; Zhuang, J.; Ding, Y.; Li, X. Optimal Design and Performance Analysis of Double Stator Multi-Excitation Flux-Switching Machine. *IEEE Trans. Appl. Supercond.* **2019**, *29*, 1–5. [CrossRef]
80. Yousuf, M.; Khan, F.; Ikram, J.; Badar, R.; Bukhari, S.S.H.; Ro, J.-S. Reduction of Torque Ripples in Multi-Stack Slotless Axial Flux Machine by Using Right Angled Trapezoidal Permanent Magnet. *IEEE Access* **2021**, *9*, 22760–22773. [CrossRef]
81. Chen, H.; Liu, X.; Demerdash, N.A.O.; El-Refaie, A.M.; Zhao, J.; He, J. Comparison and Design Optimization of a Five-Phase Flux-Switching PM Machine for In-Wheel Traction Applications. *IEEE Trans. Energy Convers.* **2019**, *34*, 1805–1817. [CrossRef]
82. Zhao, Y.; Teng, D.; Li, D.; Mi, Y.; Zhao, X. Development of Dual Armature-Winding Four-Phase Variable Flux Reluctance Generator for Fault-Tolerant Capability Improvement. *IEEE Trans. Energy Convers.* **2021**. [CrossRef]
83. Ma, C.; Qu, L.; Mitra, R.; Pramod, P.; Islam, R. Vibration and Torque Ripple Reduction of Switched Reluctance Motors through Current Profile Optimization. In Proceedings of the 2016 IEEE Applied Power Electronics Conference and Exposition (APEC), Long Beach, CA, USA, 20–24 March 2016.
84. Zhang, S.; Li, S.; Dang, J.; Harley, R.G.; Habetler, T.G. Multi-Objective Design and Optimization of Generalized Switched Reluctance Machines with Particle Swarm Intelligence. In Proceedings of the 2016 IEEE Energy Conversion Congress and Exposition (ECCE), Milwaukee, WI, USA, 18–22 September 2016.

85. Borujeni, M.M.; Rashidi, A.; Nejad, S.M.S. Optimal Four Quadrant Speed Control of Switched Reluctance Motor with Torque Ripple Reduction Based on EM-MOPSO. In Proceedings of the 6th Power Electronics, Drive Systems & Technologies Conference (PEDSTC2015), Tehran, Iran, 3–4 February 2015.
86. Namazi, M.M.; Borujeni, M.M.; Rashidi, A.; Nejad, S.M.S.; Ahn, J.-W.; Masoud, N.M. Torque Ripple Reduction of Switched Reluctance Motor Drive with Adaptive Sliding Mode Control and Particle Swarm Optimization. In Proceedings of the 2015 IEEE International Conference on Advanced Intelligent Mechatronics (AIM), Busan, Korea, 7–11 July 2015.